S1. Crystal packing

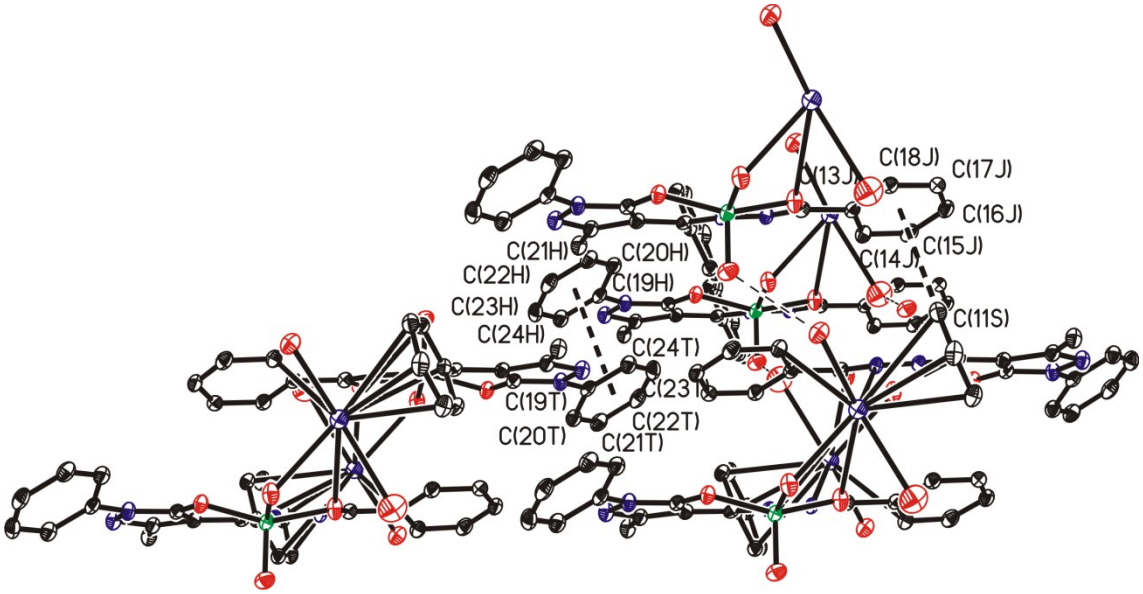

Fig. S1. Section of the crystal packing of compound $[K(H_2O)_2\{V^VO_2(bp\text{-}bhz)\}]_2$ **5.** π-π interactions between dimeric aggregates (down) with other dimeric aggregates (up) through face-to-face and edge-to-face motifs of phenyl groups are shown in dashed black lines.

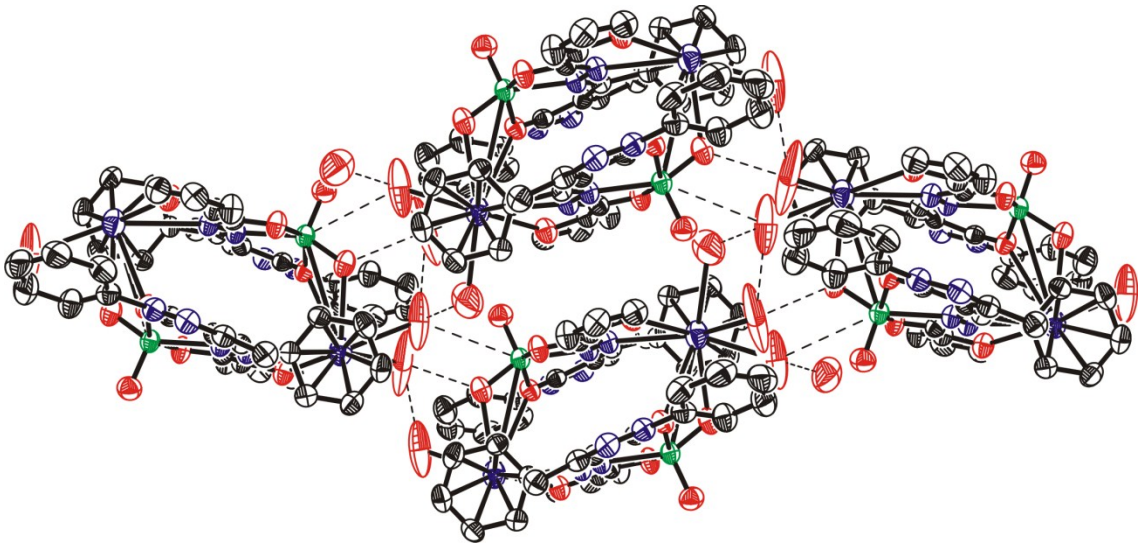

Fig. S2. Section of the crystal packing of compound $[K(H_2O)_2\{V^VO_2(bp\text{-}fah)\}]_2$ **6.** Hydrogen bonds between dimeric aggregates are shown in dashed black lines.

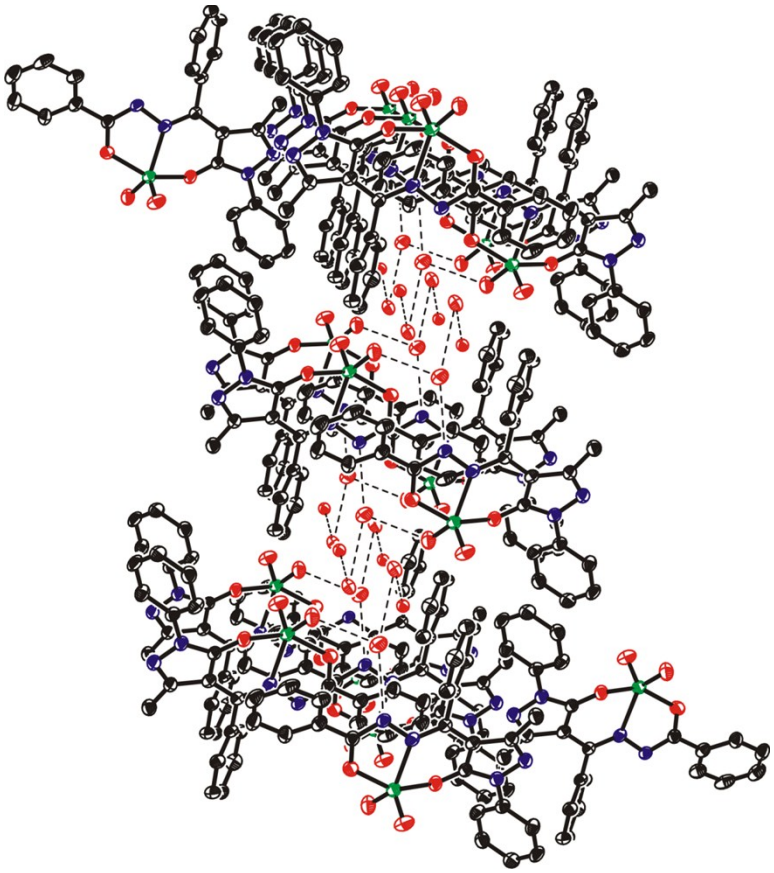

Fig. S3. Crystal packing of compound $[V^{V}O_2(Hbp\text{-}bhz)]\cdot 1.5H_2O$ **7.** Hydrogen bonds between water molecules and vanadium complexes are shown in dashed black lines.

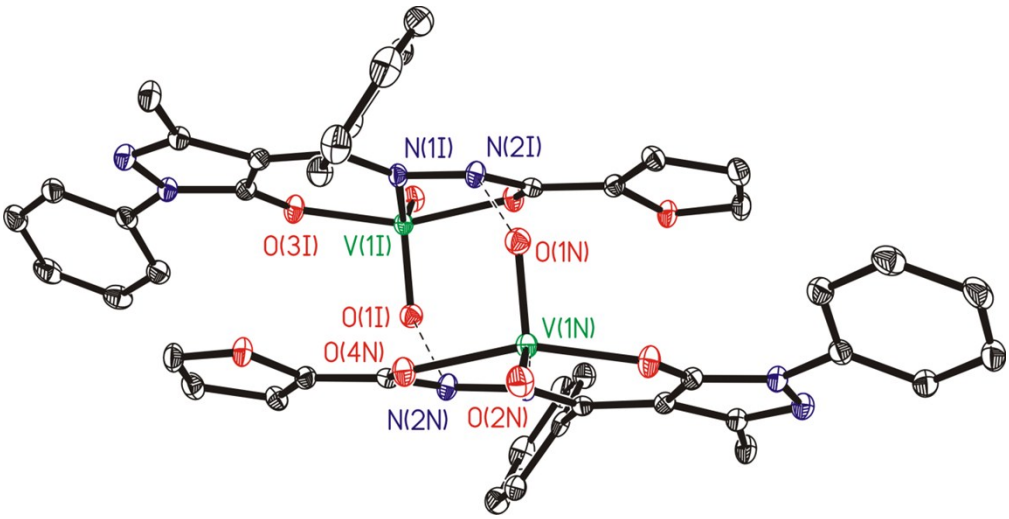

Fig. S4. Section of the crystal packing of compound $[V^{V}O_2(Hbp\text{-}fah)]$ **8.** Hydrogen bonds between terminal oxygen atoms of vanadium complexes and protonated azomethine nitrogen atoms are shown in dashed black lines.

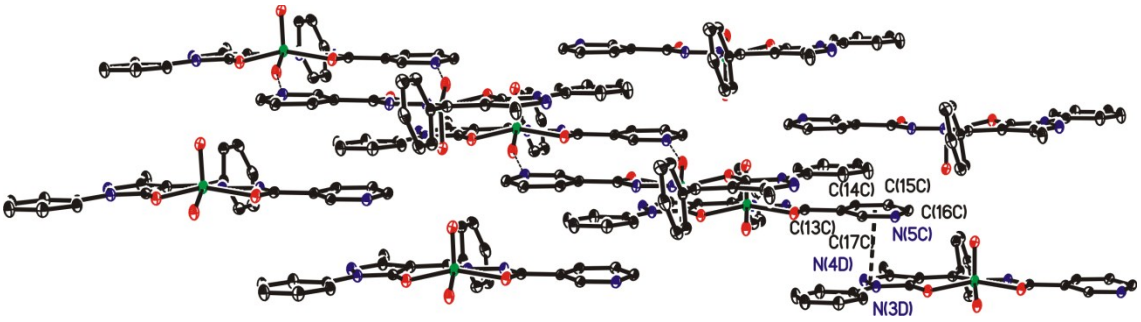

Fig. S5. Crystal packing of compound [$V^{V}O_2$(Hbp-nah)] **9.** π-π interactions between delocalized π clouds around of azomethine groups and pyridine groups are shown in dashed black lines.

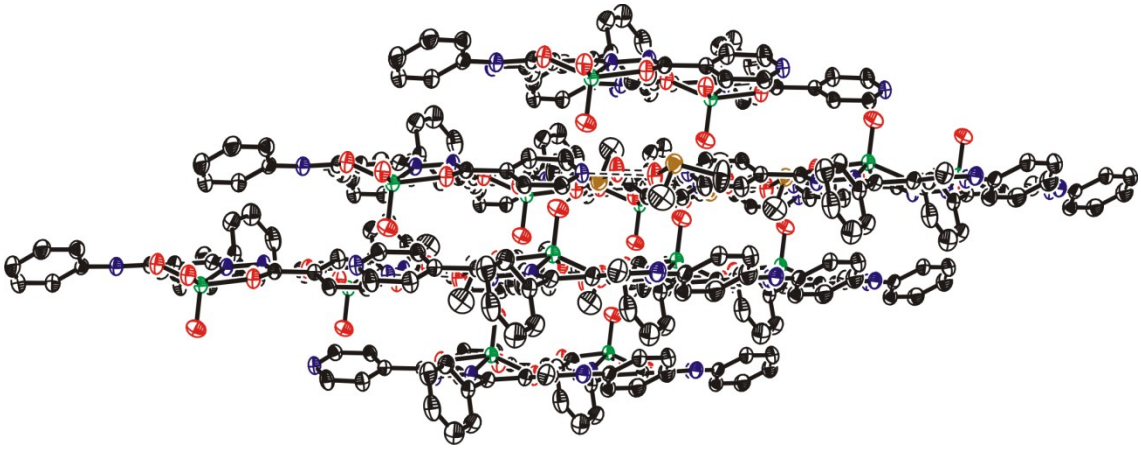

Fig. S6. Crystal packing of compound [$V^{V}O_2$(Hbp-inh)]·DMSO **10.** Layers of vanadium complexes and DMSO molecules interact by van der Waals forces.

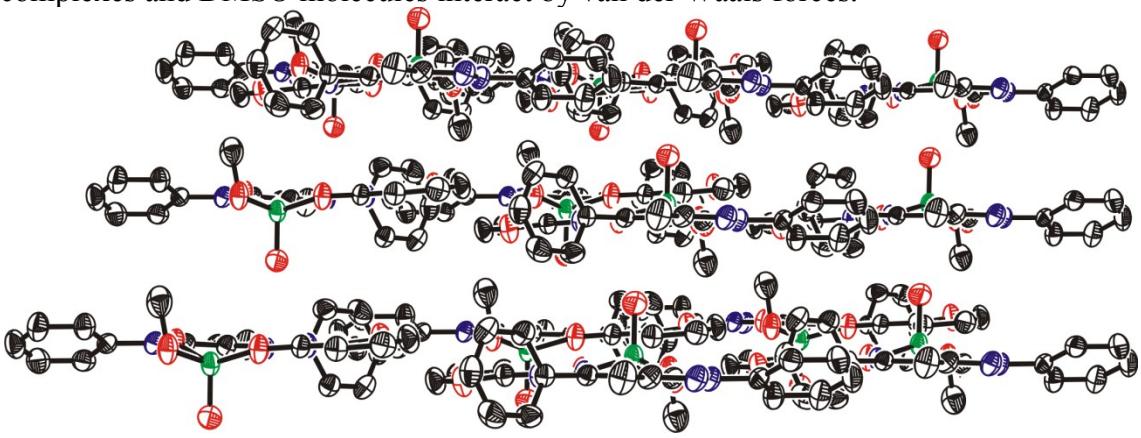

Fig. S7. Crystal packing of compound [$V^{V}O$(bp-fah)(OCH_3)] **12.** Layers of vanadium complexes interact by van der Waals forces.

S2. Solid state analysis

Table S1. Details of the thermogravimetric analysis of the complexes.

Compounds	Temp. [°C]	Obs. %	Cal. %	Expected group/Residue
$[V^{IV}O(bp\text{-}bhz)H_2O]$ **1**	125	3.5	3.7	H_2O
	497	18.9	18.8	V_2O_5
$[V^{IV}O(bp\text{-}fah)H_2O]$ **2**	112	4.0	3.8	H_2O
	521	19.8	19.3	V_2O_5
$[V^{IV}O(bp\text{-}nah)H_2O]$ **3**	114	3.8	3.7	H_2O
	489	19.2	18.8	V_2O_5
$[V^{IV}O(bp\text{-}inh)H_2O]$ **4**	121	3.6	3.7	H_2O
	500	18.2	18.8	V_2O_5
$K(H_2O)_2[V^{V}O_2(bp\text{-}bhz)]$ **5**	122	6.7	6.5	$2H_2O$
	593	24.3	25.0	KVO_3
$K(H_2O)_2[V^{V}O_2(bp\text{-}fah)]$ **6**	104	7.1	6.6	H_2O
	599	25.6	25.5	KVO_3
$[V^{V}O_2(Hbp\text{-}bhz)]$ **7**	578	18.6	19.1	V_2O_5
$[V^{V}O_2(Hbp\text{-}fah)]$ **8**	580	19.9	19.5	V_2O_5
$[V^{V}O_2(Hbp\text{-}nah)]$ **9**	583	18.8	19.0	V_2O_5
$[V^{V}O_2(Hbp\text{-}inh)]$ **10**	588	19.8	19.0	V_2O_5
$[V^{V}O(bp\text{-}bhz)(OMe)]$ **11**	125	6.4	5.9	OMe
	499	16.6	17.3	V_2O_5
$[V^{V}O(bp\text{-}fah)(OMe)]$ **12**	112	6.0	6.0	OMe
	521	16.8	17.7	V_2O_5
$[V^{V}O(bp\text{-}nah)(OMe)]$ **13**	124	6.5	5.9	OMe
	500	17.8	17.3	V_2O_5
$[V^{V}O(bp\text{-}inh)(OMe)]$ **14**	142	5.8	6.8	OMe
	501	20.3	19.6	V_2O_5

Table S2. Selected IR spectral data (ν in cm^{-1}) of ligands and complexes.

Compounds	ν (N-H)	ν (C=O) (hydrazide/pyrazolone)	ν(C-O_{enolic})	ν (C=N)	ν (N-N)	ν (V=O)/ ν(VO_2)
H_2bp-bhz **I**	3130	1644 , 1594		1539	1007	_
H_2bp-fah **II**	3127	1632 , 1593		1542	1005	_
H_2bp-nah **III**	3090	1647 , 1594		1530	1009	_
H_2bp-inh **IV**	3060	1641 , 1587		1531	1011	
[V^{IV}O(bp-bhz)H_2O] **1**		1594, 1568	1262	1520	1048	979
[V^{IV}O(bp-fah)H_2O] **2**		1608, 1562	1265	1523	1044	991
[V^{IV}O(bp-nah)H_2O] **3**		1592, 1577	1260	1522	1061	994
[V^{IV}O(bp-inh)H_2O] **4**		1598, 1580	1258	1521	1057	996
K(H_2O)$_2$[$V^{V}O_2$(bp-bhz)] **5**		1592, 1565	1259	1523	1047	934, 899
K(H_2O)$_2$[$V^{V}O_2$(bp-fah)] **6**		1606, 1564	1260	1521	1048	943, 917
[$V^{V}O_2$(Hbp-bhz)] **7**	3086	1598, 1572	-	1527	1052	937, 907
[$V^{V}O_2$(Hbp-fah)] **8**	3091	1601, 1562	-	1528	1048	925, 901
[$V^{V}O_2$(Hbp-nah)] **9**	3066	1593, 1576	1247	1522	1066	927, 899
[$V^{V}O_2$(Hbp-inh)] **10**	3051	1592, 1579	1250	1524	1055	937, 906
[V^{V}O(bp-bhz)(OMe)] **11**		1595, 1543	1256	1523	1085	968
[V^{V}O(bp-fah)(OMe)] **12**		1608, 1556	1242	1521	1081	983
[V^{V}O(bp-nah)(OMe)] **13**		1596, 1541	1251	1522	1085	982
[V^{V}O(bp-inh)(OMe)] **14**		1601, 1542	1248	1525	1089	971

S3. Characterization in solution

Table S3. UV-visible spectral data of ligands and complexes either in methanol or DMSO.

Ligand and Complexes	λ_{max} / nm (ε/ $M^{-1}cm^{-1}$)
H_2bp-bhz **I**	351 (4.81×10^4), 303 (3.61×10^4), 251 (1.48×10^4), 204(1.44×10^4)
H_2bp-fah **II**	352 (5.51×10^4), 303 (3.23×10^4), 253 (1.89×10^4), 204 (1.50×10^4)
H_2bp-nah **III**	358 (4.73×10^4), 305 (2.84×10^4), 250 (1.54×10^4), 205 (1.35×10^4)
H_2bp-inh **IV**	368 (4.96×10^4), 306 (2.96×10^4), 251 (1.64×10^4), 205 (1.41×10^4)
[V^{IV}O(bp-bhz)(H_2O)] **1**	654 (1.4×10^2)), 480 (1.7×10^2), 398 (1.34×10^3), 341 (3.33×10^4), 245 (2.32×10^4), 205 (5.43×10^4)
[V^{IV}O(bp-fah)(H_2O)] **2**	667 (2.1×10^2), 509 (2.6×10^2), 388 (2.32×10^3), 325(3.03×10^3), 242 (3.43×10^4), 206 (1.22×10^4)
[V^{IV}O(bp-nah)(H_2O)] **3**	645 (1.7×10^2), 486 (2.2×10^2), 389(2.32×10^3), 326 (1.23×10^4), 244 (3.24×10^3), 207(1.51×10^3)
[V^{IV}O(bp-inh)(H_2O)] **4**	650 (1.5×10^2), 480 (1.9×10^2), 397 (1.51×10^3), 338 (4.65×10^4), 235 (2.13×10^4), 205 (1.18×10^4)
$K(H_2O)_2$[V^VO_2(bp-bhz)] **5**	401 (3.13×10^3), 342 (2.12×10^4), 241 (1.45×10^4), 205 (1.98×10^4)
$K(H_2O)_2$[V^VO_2(bp-fah)] **6**	394 (2.78×10^3), 346 (3.13×10^4), 248 (2.34×10^4), 207 (2.12×10^4)
[V^VO_2(Hbp-bhz)] **7**	402 (2.32×10^3), 345(1.18×10^4), 243 (3.39×10^4), 204 (4.21×10^4)
[V^VO_2(Hbp-fah)] **8**	404 (2.67×10^3), 366 (2.32×10^4), 249 (1.78×10^4), 205 (4.12×10^4)
[V^VO_2(Hbp-nah)] **9**	388 (4.12×10^3), 341 (3.05×10^4), 243 (2.13×10^4), 207 (3.12×10^4)
[V^VO_2(Hbp-inh)] **10**	393(1.45×10^3), 341 (6.32×10^4), 235 (2.48×10^4), 206 (3.09×10^4)
[V^VO(bp-bhz)(OMe)] **11**	394 (2.13×10^3), 341 (3.02×10^4), 245 (2.67×10^4), 206 (2.56×10^4)
[V^VO(bp-fah)(OMe)] **12**	401(2.34×10^3), 309(3.56×10^3), 248 (3.12×10^4), 207 (2.33×10^4)
[V^VO(bp-nah)(OMe)] **13**	397(3.45×10^3), 351(2.12×10^4), 258(2.34×10^3), 209(2.12×10^3)
[V^VO(bp-inh)(OMe)] **14**	399 (2.13×10^3), 347 (3.23×10^4), 262 (1.87×10^4), 205 (2.11×10^4)

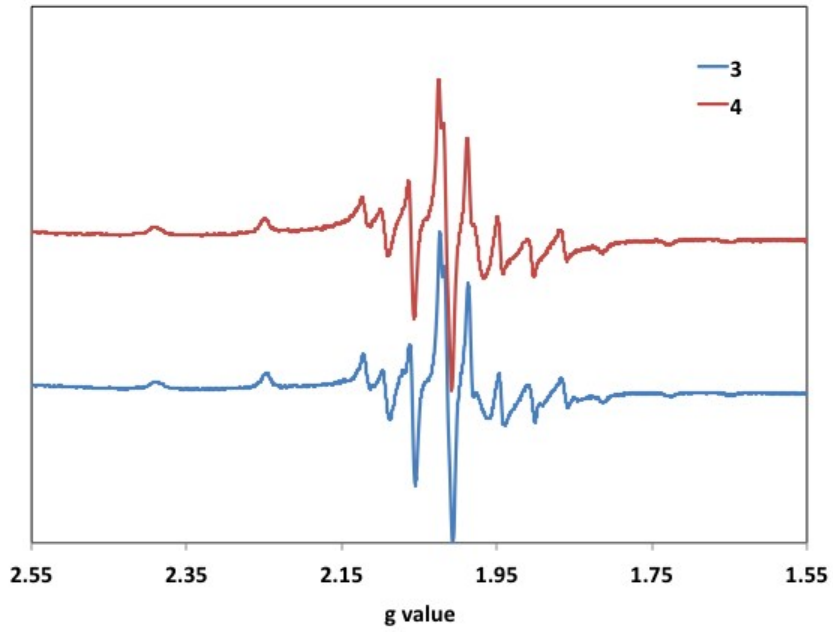

Fig. S8. X-band EPR spectra measured at 77K for the $V^{IV}O$-complexes **3** and **4** dissolved in DMSO.

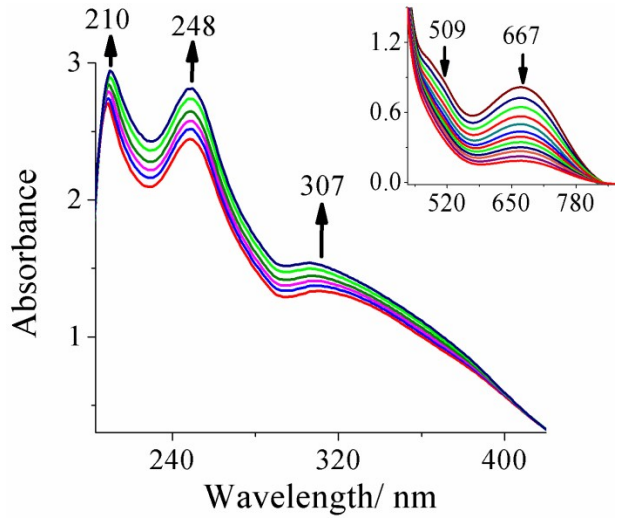

Fig. S9. UV-Vis spectral changes observed during titration of $[V^{IV}O(bp\text{-}fah)H_2O]$ **2** with H_2O_2. The spectra were recorded upon stepwise additions of one drop portions of H_2O_2 (3.1×10^{-2} M) to 25 mL of 4.2×10^{-4} M solution of **2** in DMSO. The inset shows spectral changes observed for the d-bands of complex **2** in DMSO upon addition of H_2O_2. The spectra were recorded upon

stepwise addition of two drop portions of H_2O_2 (3.6×10^{-2} M) to 25 mL of a 3.3×10^{-3} M solution of **2** in DMSO.

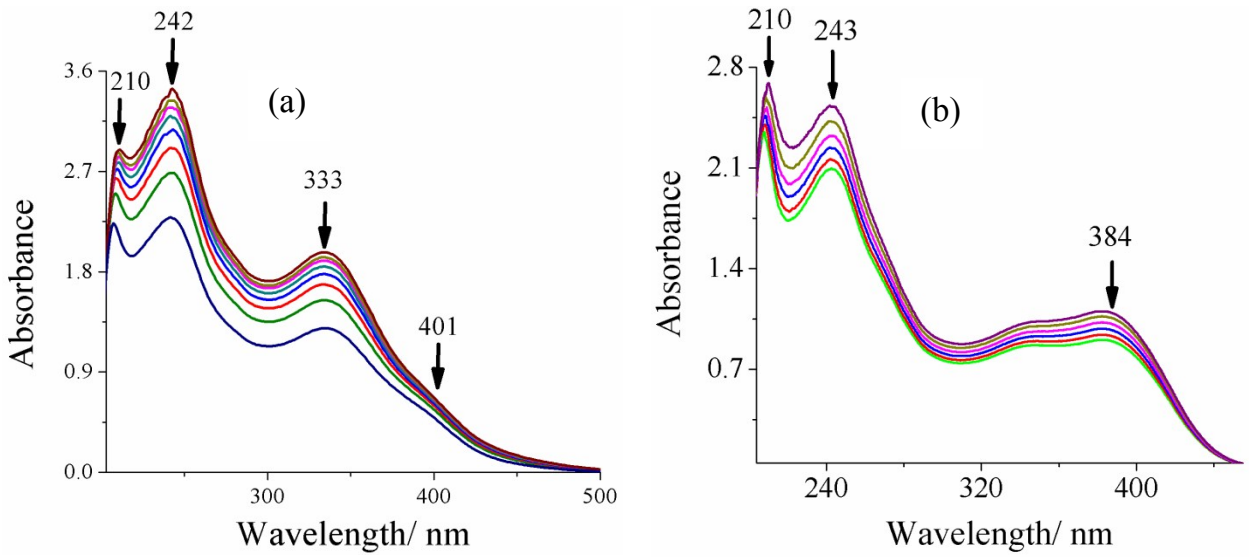

Fig. S10. (a) Spectral changes observed during titration of [V^VO_2(Hbp-nah)] **9** with H_2O_2. The spectra were recorded upon stepwise addition of one drop portions of 1.2×10^{-2} M H_2O_2 to 25 mL of 1.3×10^{-4} M solution in CH_3OH. (b) Spectral changes observed during titration of [V^VO_2(Hbp-inh)] **10** with H_2O_2. The spectra were recorded upon stepwise addition of one drop portions of 2.5×10^{-2} M H_2O_2 to 25 mL of 2.2×10^{-4} M solution in CH_3OH.

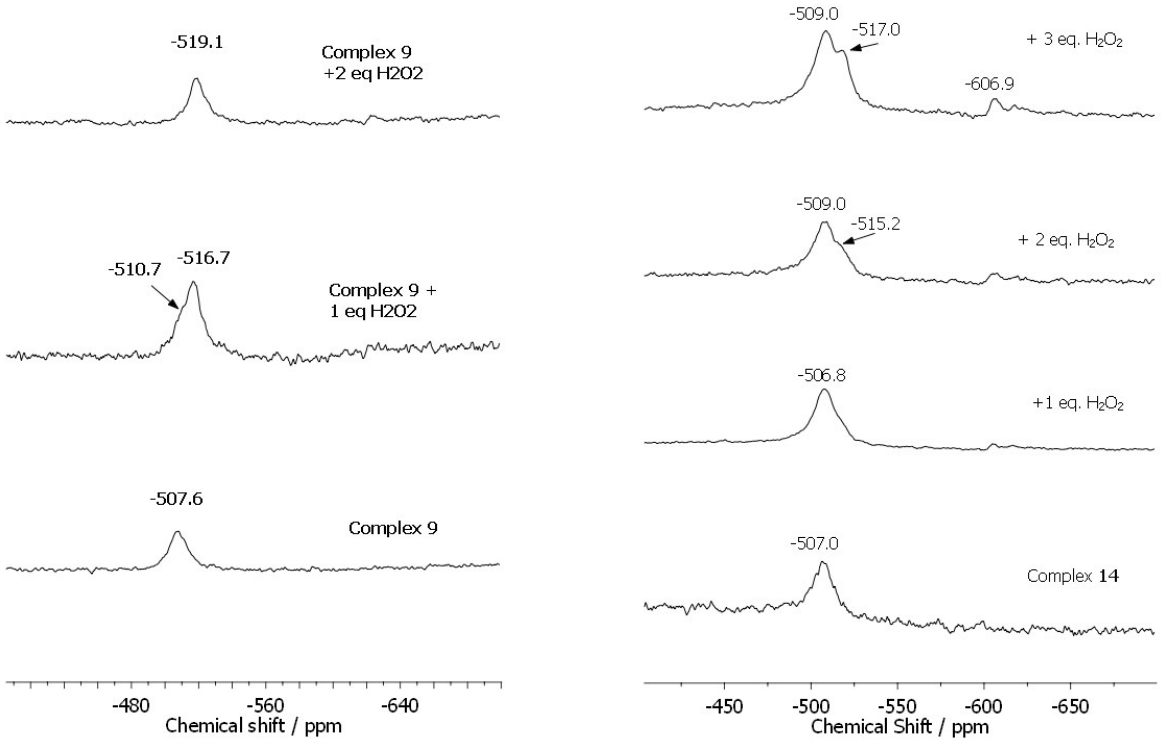

a) b)

Fig. S11. ^{51}V NMR spectra measured for 3mM solutions of the complexes in DMSO, before and after addition of different amounts of H_2O_2. a) Complex **9** and b) complex **14**.

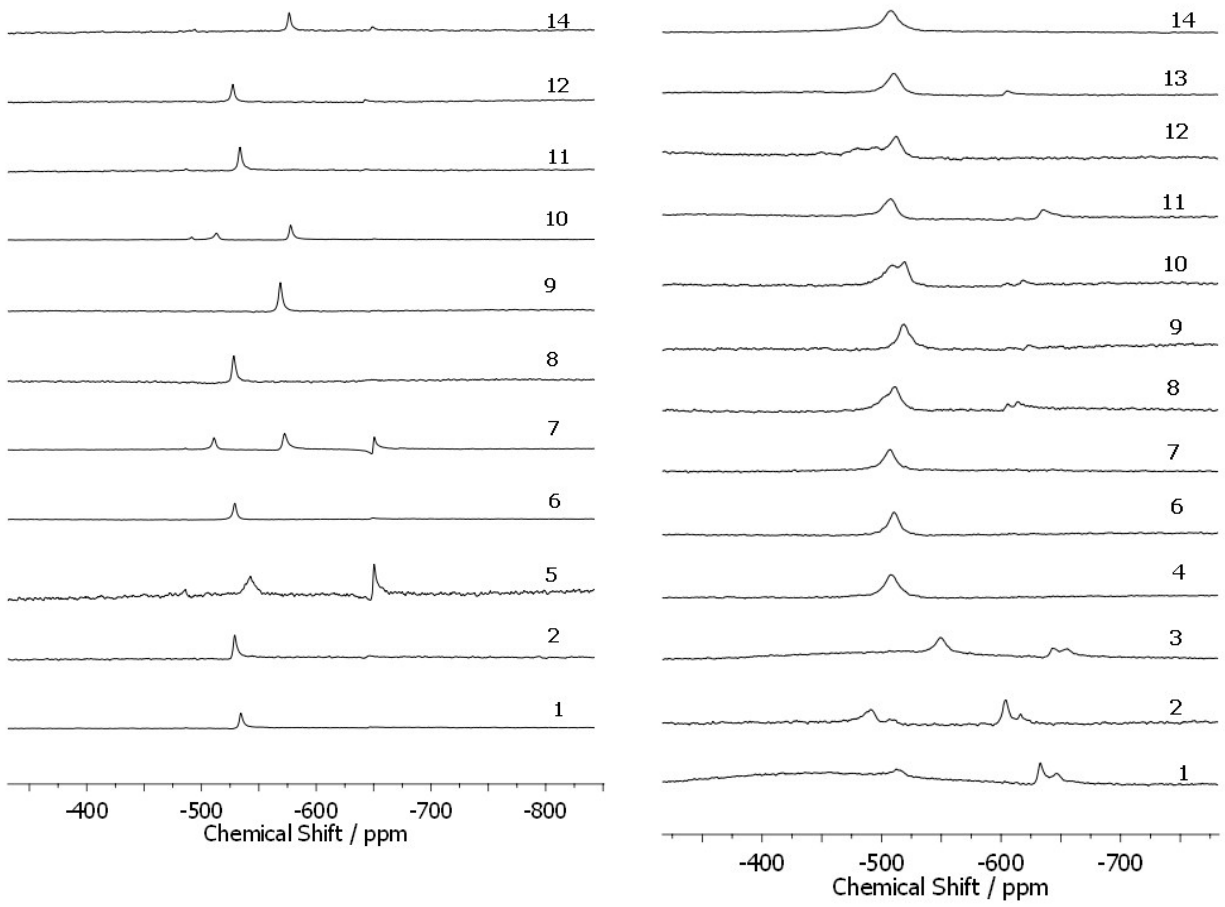

a) **b)**

Fig. S12. ^{51}V NMR spectra measured for 3mM solutions of the complexes after addition of H_2O_2. a) in MeOH and b) in DMSO.

S4. Catalytic studies

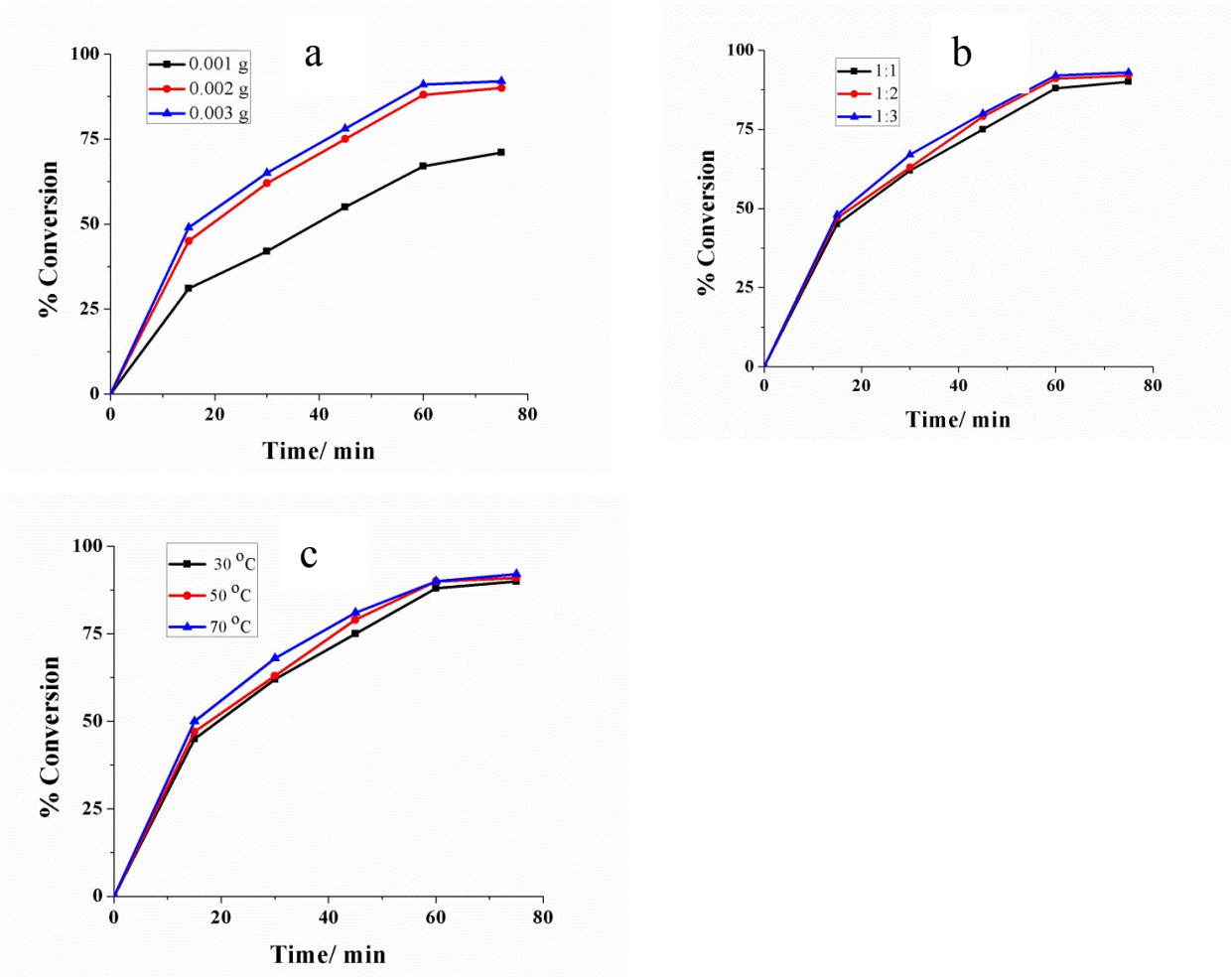

Fig. S13. (**a**) Effect of amount of catalyst [[$V^{V}O$(bp-bhz)(OMe)] on the multi-component Hantzsch reaction. Reaction conditions: benzaldehyde (0.53 g, 0.0050 mol), ethylacetoacetate (0.010 mol, 1.3 g), ammonium acetate (0.38 g, 0.0050 mol) and H_2O_2 (0.56 g, 0.0050 mol) at 30 °C. (**b**) Effect of different substrate/oxidant ratios on the Hantzsch reaction. Reaction conditions: benzaldehyde (0.53 g, 0.0050 mol), ethylacetoacetate (1.3 g, 0.010 mol), ammonium acetate (0.38 g, 0.0050 mol,) and catalyst (0.0020 g) at 30 °C. (**c**) Effect of the temperature on the Hantzsch reaction. Reaction conditions: benzaldehyde (0.53 g, 0.0050 mol), ethylacetoacetate (1.3 g, 0.010 mol), ammonium acetate (0.38 g, 0.0050 mol), H_2O_2 (0.56 g, 0.0050 mol) and catalyst (0.0020 g).

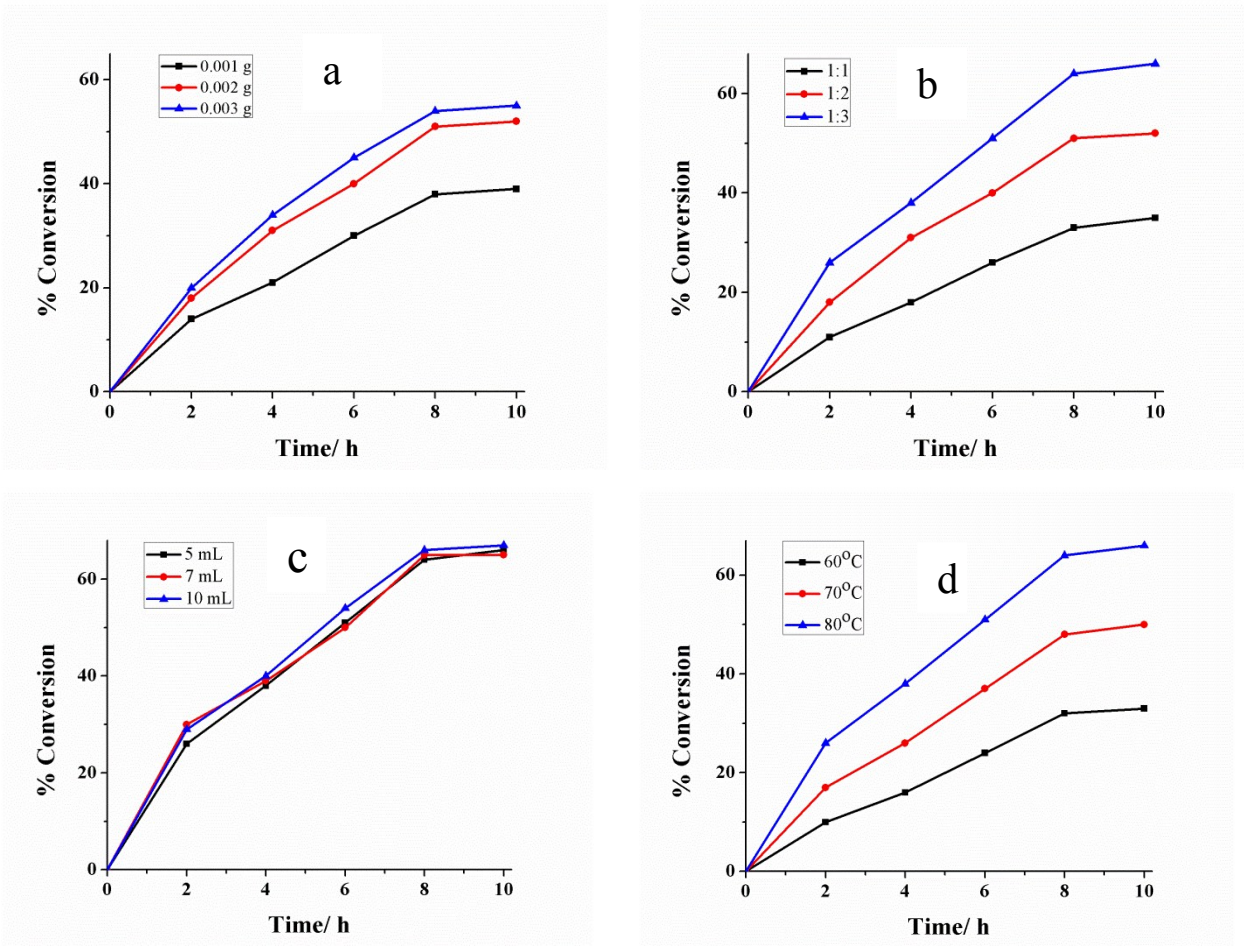

Fig. S14. (**a**) Effect of amounts of catalyst [$V^{V}O$(bp-bhz)(OMe)] on the oxidation of tetralin. Other reaction conditions: tetralin (1.3 g, 0.010 mol), 30% H_2O_2 (2.3 g, 0.020 mol), acetonitrile (5 mL) and reaction temp. (80°C)]. (**b**) Effect of substrate/oxidant ratios on the oxidation of tetralin. Other reaction conditions: tetralin (1.3 g, 0.010 mol), catalyst (0.0020 g), acetonitrile (5 mL) and reaction temp. (80 °C). (**c**) Effect of amounts of solvent on the oxidation of tetralin. Other reaction conditions: tetralin (1.3 g, 0.010 mol), catalyst (0.0020 g), 30% H_2O_2 (3.4 g, 0.030 mmol) and reaction temp. (80 °C). (**d**) Effect of variation of temperature on the oxidation of tetralin. Other reaction conditions: tetralin (1.3 g, 0.010 mol), catalyst (0.0020 g), 30% H_2O_2 (3.4 g, 0.030 mol and acetonitrile (5 mL).